Mutagenesis Studies toward Understanding the Mechanism of Differential Reactivity of Factor Xa with the Native and Heparin-Activated Antithrombin†

Alireza R. Rezaie,* Likui Yang, and Chandrashekhara Manithody

Edward A. Doisy Department of Biochemistry and Molecular Biology, Saint Louis University School of Medicine, Saint Louis, Missouri 63104

Received November 29, 2003; Revised Manuscript Received January 21, 2004

ABSTRACT: A unique pentasaccharide fragment of high-affinity heparin activates antithrombin (AT) to enhance its rate of complex formation with factor Xa (FXa) by 200−300-fold. Recent results have indicated that the activation of AT is associated with the exposure of a cryptic exosite on the serpin that is an interactive site for FXa in the complex. Previously, we identified Arg^{150} on the autolysis loop of FXa as a candidate residue that may specifically interact with the heparin-activated AT. Three other surface loops on FXa including 39, 60, and the sodium-binding 220 loops have been implicated to be critical for the protease interaction with the activated AT. To determine the extent of the contribution of these loops to the specificity of the FXa interaction with activated AT, several loop mutants of the protease were prepared and their reactivity with AT was studied in both the absence and presence of pentasaccharide. Analysis of the inhibition kinetic data suggests that the residues of both 39 and 60 loop make a minor contribution to the recognition of AT in both the native and activated conformation of the serpin. On the other hand, the reactivity of AT with the sodium loop mutants of FXa in the absence of the cofactor was severely impaired. However, the extent of the rate-accelerating effect of pentasaccharide in the AT inhibition of the mutants was not affected. These results suggest that all three loops play a role in the specificity of the FXa−AT interaction; however, neither loop specifically interacts with the activated conformation of the serpin.

Factor Xa (FXa)[1] is a vitamin K-dependent coagulation serine protease, which upon complex formation with other components of the prothrombinase complex (factor Va, negatively charged membrane and calcium) converts prothrombin to thrombin at a high rate in the final stage of the blood coagulation cascade (*1*−*3*).[2] The proteolytic activity of FXa is primarily regulated by antithrombin (AT), which is a serpin capable of forming a 1:1 stoichiometric inactive complex with coagulation serine proteases of both intrinsic and extrinsic pathways (*4*−*6*). Unlike other serpins, AT exhibits a lower reactivity toward its target proteases unless it is activated by the physiologically relevant heparin-like glycosaminoglycans found on the surface of the endothelium (*7*, *8*). Heparin-activated AT inhibits FXa (and also FIXa) with a 200−300-fold enhanced rate constant (*9*−*11*). The mechanism by which heparin activates AT to improve its reactivity with the coagulation proteases has been extensively studied in recent years. Structural and mutagenesis data both have indicated that in the absence of heparin, the N-terminal P14 and P15 residues of the AT reactive center loop (RCL) are inserted into the major central β-sheet A of the serpin (*12*−*14*). It was initially thought that this structural feature causes a disordered RCL structure for the serpin that is incapable of fitting into the catalytic pocket of FXa. On the basis of distinct structural changes in AT upon complex formation with pentasaccharide, including the observation that the partially inserted RCL was expelled out of β-sheet A, it was hypothesized that a cofactor-mediated conformational change in RCL activates the serpin by optimizing the complementarity of the loop for docking into the catalytic pocket of FXa (*9*, *12*, *15*). Although recent mutagenesis data supported these structural changes associated with AT upon interaction with pentasaccharide (*13*, *16*), they nevertheless did not confirm the conclusion that a conformational change in RCL is solely responsible for the rate-accelerating effect of the cofactor in protease inhibition by the serpin (*17*). This was evidenced by the observation that the mutagenesis of any one of the P6−P3′ residues of the loop had minimal effect in the extent of the rate-accelerating effect of pentasaccharide in FXa inhibition by mutant serpins (*17*). Thus, a revised model for the mechanism of the AT activation by heparin has been proposed which hypothesizes that the cofactor-mediated structural changes in serpin are coupled

† The research was supported by grants awarded by the National Heart, Lung, and Blood Institute of the National Institutes of Health (HL 62565 and HL 68571 to A.R.R.).

* To whom correspondence should be addressed: Alireza R. Rezaie, Ph.D. Department of Biochemistry and Molecular Biology, St. Louis University School of Medicine, 1402 S. Grand Blvd., St. Louis, MO 63104. Phone: (314) 977-9240. Fax: (314) 977-9205. E-mail: rezaiear@slu.edu.

[1] Abbreviations: FXa, factor Xa; GD-FXa, Gla-domainless factor Xa; FIXa, factor IXa; AT, antithrombin; RCL, reactive center loop; SpFXa, spectrozyme FXa.

[2] Nomenclature of Schechter and Berger (*1*) used to describe the subsites of interaction between a protease and its substrate. Amino acid residues of the substrate are referred to as P1, P2, etc., on the N-terminal side of the substrate scissile bond and those on the C-terminal side are referred to as P1′, P2′, etc. The corresponding sites on the enzyme where substrate residues interact are designed S1, S2, ...and S1′, S2′, ..., respectively.

10.1021/bi036145a CCC: $27.50
Published on Web 02/19/2004

to the exposure of a cryptic exosite outside of the P6−P3′ site of RCL that interacts with a complementary exosite of FXa remote from the catalytic pocket (*17*). In support of this hypothesis, in a recent mutagenesis study, the same authors identified the strand 3 of β-sheet C on AT as the protease interactive site that may be responsible for the rate-accelerating effect of both FIXa and FXa inhibition by the activated serpin (*18*).

Additional support for an exosite-dependent interaction between heparin activated conformation of AT and FXa was provided by our recent observation that the conserved basic residue, Arg^{150} (chymotrypsinogen numbering (*19*)), on the autolysis loop of both FIXa and FXa specifically interacts with the activated conformation of the serpin (*20, 21*). This was evidenced by the observation that the substitution of Arg^{150} with an Ala in both proteases resulted in mutants that exhibited near normal reactivity with AT in the absence of pentasaccharide, but an order of magnitude impaired reactivity with the serpin in the presence of the cofactor (*20, 21*). However, noting an ∼200−300-fold higher reactivity of the heparin activated AT with FXa relative to the native serpin, the interaction of the autolysis loop with the activated conformation of AT does not account for all of the rate-accelerating effects of the polysaccharide in the protease inhibition by the serpin. Thus, in addition to the autolysis loop, it has been reported that other AT interactive sites, including residues on 39, 60 (*22*), and the sodium-binding 220 loops (*17*), may exist on FXa that can specifically interact with the activated conformation of the serpin. Moreover, a previously published molecular model of the activated AT−FXa complex has predicted that the 39 loop of FXa may interact with a basic site on AT composed of several basic residues including Lys^{403} and Lys^{406} (*23*). To further investigate these questions, we prepared a Lys^{403} → Thr mutant of AT and several mutants of FXa in which the variant residues of all three surface loops including Glu^{36}, Glu^{37}, and Glu^{39} of the 39 loop; Gln^{61}, Lys^{62}, and Arg^{63} of the 60 loop; and Arg^{221}, Lys^{222}, and Lys^{224} of the sodium-binding 220 loop were either substituted with Gln, Ala, or their charges were reversed. Following expression, purification, and activation of FX derivatives by the FX activating enzyme from Russell's viper venom, the reactivity of the mutants with AT was analyzed in both the absence and presence of pentasaccharide. It was discovered that with the exception of the sodium-binding loop mutants of FXa, all other mutants showed minor changes in their reactivity with AT in either the absence or presence of pentasaccharide. Although the reactivity of the 220 loop mutants of FXa with AT was severely impaired, the extent of the rate-accelerating effect of pentasaccharide in the AT inhibition of mutants was, nonetheless, not negatively affected. These results suggest that although residues of all three surface loops contribute to the determination of the specificity of FXa−AT interaction, neither one is specific for interaction with the activated serpin. These results, in the context of the molecular model of the activated AT−FXa Michaelis complex (*23*), are discussed.

MATERIALS AND METHODS

Construction, Mutagenesis, and Expression of Recombinant Proteins. The construction and expression of recombinant wild type factor X (FX) in both the full-length and Gla-domainless forms (GD-FX) in human embryonic kidney 293 cells have been described previously (*20*, *24*). The FX mutants in which Glu^{36} → Gln(E36Q), Glu^{37} → Gln(E37Q), Glu^{39} → Gln or Ala (E39Q and E39A), Gln^{61} → Ala (Q61A), Lys^{62} → Glu (K62E), Arg^{63} → Glu (R63E) were substituted with indicated residues, were prepared by PCR mutagenesis methods and expressed in the same vector system as described (*20*). The Na^+-binding loop mutant of FX in the GD-FX form in which the two residues Ala^{220} and Lys^{222} were replaced with two Asp residues found at the corresponding sites of thrombin was prepared by the same methods and expressed in the same expression/purification vector system as described above. The substitution of these two residues results in a FX mutant ($220-225^{Th}$) in which the 220−225 loop of the protease is identical to the corresponding sequence of thrombin. Thrombin, unlike FXa, does not differentiate between the native and activated conformations of AT. Another Na^+-loop mutant was prepared in which the three basic residues Arg^{221}, Lys^{222}, and Lys^{224} were substituted with Ala (R221A/K222A/K224A). Wild-type AT and an AT mutant in which Lys^{403} of the serpin was replaced with a Thr (K403T) was also constructed and expressed in the same mammalian cells as described (*25*). The accuracy of all constructs was confirmed by DNA sequencing prior to their expression in mammalian cells. The construction, expression, and characterization of the autolysis loop mutants of FX including Arg^{143} → Ala (R143A), Lys^{147} → Ala (K147A), Arg^{150} → Ala (R150A), and Arg^{154} → Ala (R154A), has been described previously (*20*). All mutants were purified to homogeneity, activated by the FX activating enzyme from Russell's viper venom (RVV-X), and active-site titrated with known concentrations of AT as described (*20*, *26*). AT concentrations were determined from the absorbance at 280 nm using a molar absorption coefficient of 37 700 M^{-1} cm^{-1} and by stoichiometric titration of the serpin with the calibrated heparin as monitored from changes in intrinsic protein fluorescence as described (*27*).

Human plasma FXa and RVV-X were purchased from Haematologic Technologies Inc. (Essex Junction, VT). The active AT-binding pentasaccharide fragment of heparin (fondaparinux sodium) was purchased from Quintiles Clinical Supplies (Mt. Laurel, NJ). A full-length high-affinity heparin with an average molecular mass of ∼21 000 (∼70 saccharides) was a generous gift from Dr. Steven Olson (University of Illinois-Chicago). Concentrations of heparins were based on the AT-binding sites and were determined by stoichiometric titration of AT with the polysaccharides, with monitoring of the interaction by changes in protein fluorescence as described (*27*). The chromogenic substrates, Spectrozyme FXa was purchased from American Diagnostica (Greenwich, CT), and S2765 was purchased from Kabi Pharmacia/Chromogenix (Franklin, OH).

Cleavage of Chromogenic Substrates by the Factor Xa Derivatives. The steady-state kinetics of hydrolysis of SpFXa (7.8−1000 μM) and S2765 (0.04−5.0 mM) by the FXa derivatives (0.5 nM for all mutants with the exception of 25 nM for the sodium-binding loop mutants) were measured in 0.1 M NaCl, 0.02 M Tris-HCl (pH, 7.5) containing 0.1 mg/mL bovine serum albumin, 0.1% poly(ethylene glycol) 8000, and 5 mM Ca^{2+} (TBS/Ca^{2+}) at 405 nm at room temperature by a V_{max} Kinetic Microplate reader (Molecular Devices, Menlo Park, CA) as described (*20*). The K_m and k_{cat} values

for the substrate hydrolysis were calculated from the Michaelis−Menten equation as described (*20*).

Fluorescence Measurements. An Aminco-Bowman series 2 spectrophotometer (Spectronic Unicam, Rochester, NY) was used for protein fluorescence measurements at 25 °C. The excitation and emission wavelengths were 280 and 340 nm, respectively. The bandwidths were set at 1 nm for excitation and 8 nm for emission. Pentasaccharide titration was performed by addition of 2−4 μL of high concentration stock solution of fondaparinux sodium (H_5) into 50 nM of each AT sample in 20 mM Tris-HCl, 0.1 M NaCl, and 0.1% PEG 8000, pH 7.5. Following titration with H_5, the ratio of changes in the fluorescence intensity of the AT sample containing H_5 to the initial intensity of the control protein lacking H_5 was calculated and plotted as a function of H_5 concentrations. The affinity of AT for H_5 was calculated by nonlinear least-squares computer fitting of the data by the quadratic binding equation as described (*27*).

Inhibition Assays. The rate of inhibition of the FXa derivatives by AT in both the absence and presence of H_5 was measured under pseudo-first-order rate conditions by a discontinuous assay method as described (*28*). In the absence of the cofactor, FXa (1 nM for all mutants with the exception of 25 nM for the sodium loop mutants) was incubated with 125−2000 nM human AT in TBS/Ca^{2+} at room temperature in 50 μL volumes in 96-well polystyrene plates. In the presence of H_5, the reaction conditions were the same except that the rate of enzyme inhibition (0.5 nM for all mutants and 10 nM for the sodium loop mutants) was monitored at a fixed concentration of AT (0.5−2 μM) and varying concentrations of the cofactor (5−50 nM for all mutants with the exception of 125−1000 nM for the sodium loop mutants). To determine the kinetic basis for the dramatic impairment in the reactivity of the sodium loop mutants of FXa with AT, the inactivation of the R221A/K222A/K224A mutant by AT was also studied in the presence of a full-length high affinity heparin. In this case, the rate of the mutant enzyme (10 nM) inhibition by AT (1−5 μM) was monitored in the presence of increasing concentrations of heparin (0.08−2.56 μM). After a period of time (30 s to 80 min depending on the rate of reaction), 50 μL of SpFXa or S2276 (0.5−1.0 mM) in TBS was added to each well and the remaining enzyme activity was measured with a V_{max} Kinetics Microplate reader. The observed pseudo-first-order rate constants (k_{obs}) were determined by fitting data to an exponential loss of activity with a zero endpoint. The second-order association rate constants for uncatalyzed and catalyzed reactions were obtained from the slopes of linear plots of k_{obs} vs the concentration of AT or the AT−heparin complex, respectively, in accordance with eq 1, as described (*27*).

$$k_{obs} = k_{uncat}[AT]_{free} + k_H[AT{-}heparin] \qquad (1)$$

In this equation k_{uncat} and k_H are the second-order rate constants for uncatalyzed and heparin-catalyzed reactions, respectively, $[AT]_{free}$ and [AT−heparin] represent the free and AT−heparin complex concentrations, which were calculated from the dissociation constant for the AT−heparin (or pentasaccharide) interaction and total concentrations of AT ($[AT]_o$) and heparin ($[H]_o$) using the quadratic eq 27.

In inhibition reactions where the k_{obs} values exhibited a saturable dependence on the concentrations of the AT−heparin complex, data were analyzed according to the hyperbolic eq 2 as described (*27*, *28*).

$$k_{obs} = k[AT{-}heparin]/K_D + [AT{-}heparin] \qquad (2)$$

In this equation k represents the limiting rate constant for the conversion of the intermediate heparin−AT−protease ternary encounter complex to a stable AT−protease complex; K_D is the dissociation constant for binding of the protease to the AT−heparin complex to form the ternary complex.

RESULTS AND DISCUSSION

Expression and Purification and Activation of Recombinant Proteins. Both wild type and mutant FX derivatives were expressed in the universal expression/purification vector systems as described (*20*, *24*). The mutant proteins were purified to homogeneity by a combination of immunoaffinity and ion exchange chromatography using the monoclonal antibody HPC4 and a Mono Q column as described (*20*). SDS−PAGE analysis of all FX derivatives suggested that the recombinant proteins have been purified to homogeneity and that they all migrate with similar molecular masses as the plasma-derived FX (data not shown). All derivatives could be converted to their active forms by RVV-X as determined by an amidolytic activity assay using SpFXa or S2765. Following activation, the concentration of FXa derivatives were determined by both an amidolytic activity assay and active-site titration with known concentrations of AT as described (*20*, *26*). These concentrations were within 80−100% of those expected based on zymogen concentrations as determined from the absorbance at 280 nm. Some of the mutants, including those of the sodium-binding 220 loop mutants, were constructed in the Gla-domainless forms since, unlike full-length FX, GD-FX expresses to a high yield in mammalian cells. Thus, FX derivatives containing multiple mutations were expressed as GD-FX forms. We have extensively studied the inhibition profile of GD-FXa by AT in the absence and presence of different derivatives of heparin (29). Both full-length FXa and GD-FXa react with AT with indistinguishable kinetics in both the absence and presence of heparin cofactors in TBS containing physiological levels of Ca^{2+} (*29*). We previously showed that the Ca^{2+} stabilization of the Gla domain of FXa is required for the ability of the protease to interact with heparin (*30*). In the absence of Ca^{2+}, the template effect of full-length heparin in the AT inhibition of FXa is abolished, possibly due to the masking of the heparin binding exosite of FXa by the misfolded acidic Gla domain (*30*). Both full-length FXa and GD-FXa also exhibit similar activity toward chromogenic substrates. Thus, both forms of FXa derivatives are suitable for studying the kinetics of the protease inhibition by AT in the absence and presence of heparin cofactors.

Both the wild type and the K403T mutant of AT were purified by a combination of immunoaffinity and Hitrap-Heparin column chromatography as described (*25*). SDS−PAGE analysis suggested that both proteins have been purified to homogeneity (data not shown). The interaction of heparin with AT is associated with a 30−40% enhancement in the intrinsic protein fluorescence of the serpin (*27*). Fluorescence measurements indicated that pentasaccharide (fondaparinux sodium) binds to wild type and mutant AT with K_D values of 12.4 ± 3.9 and 18.9 ± 6.9 nM, respectively

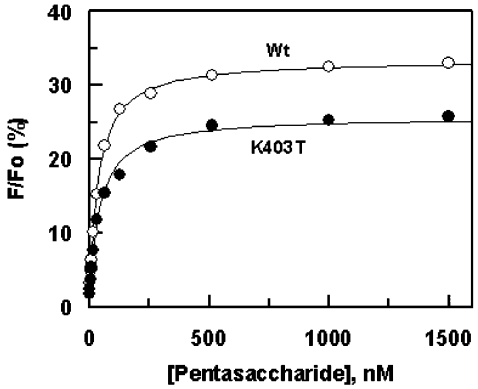

FIGURE 1: Binding of pentasaccharide (fondaparinux sodium) to recombinant AT derivatives. Pentasaccharide-induced spectral changes were monitored at room temperature by stepwise addition of 2−4 μL of a concentrated stock solution of heparin to 50 nM of each AT derivative in 20 mM Tris-HCl, 0.1 M NaCl, and 0.1% PEG 8000, pH 7.5. Dissociation constant for each derivative was calculated from the changes of the intrinsic protein fluorescence by nonlinear regression analysis using the quadratic equation for the tight binding interactions as described under Materials and Methods. The symbols are (○) wild type, (●) K403T.

Table 1: Kinetic Constants for the Cleavage of Spectrozyme FXa and S2765 by FXa Derivatives[a]

spectrozyme FXa	K_m (μM)	k_{cat} (s^{-1})	k_{cat}/K_m ($\mu M^{-1} s^{-1}$)
FXa	74.8 ± 3.8	136.5 ± 2.5	1.8 ± 0.1
E36Q	79.7 ± 4.2	160.4 ± 3.3	2.0 ± 0.1
E37Q	80.5 ± 3.7	148.0 ± 2.5	1.8 ± 0.1
E39Q	85.9 ± 4.8	163.7 ± 3.3	1.9 ± 0.1
E39A	63.5 ± 4.9	120.9 ± 2.5	1.9 ± 0.2
Q61A	80.6 ± 3.4	125.0 ± 1.6	1.6 ± 0.1
K62E	67.2 ± 2.3	153.0 ± 1.6	2.3 ± 0.1
R63E	67.0 ± 3.2	131.6 ± 2.1	2.0 ± 0.1
GD-FXa	76.1 ± 4.1	138.2 ± 2.0	1.8 ± 0.1
S2765			
GD-FXa	49.5 ± 1.8	235.9 ± 3.0	4.8 ± 0.2
220−225Th	1100 ± 100	4.5 ± 0.2	0.004 ± 0.0005
R221A/ K222A/ K224A	4100 ± 200	3.1 ± 0.1	0.0008 ± 0.0001

[a] The kinetic constants were calculated from the cleavage rate of increasing concentrations of SpFXa and S2765 by FXa and GD-FXa derivatives, respectively, in TBS/Ca^{2+} at room temperature as described under Materials and Methods.

(Figure 1). Thus, the ability of the mutant to interact with the synthetic cofactor was slightly impaired (less than 2-fold). This may reflect the slightly lower pentasaccharide-mediated fluorescent enhancement observed with the AT mutant (Figure 1). Similar to the reaction of wild-type FXa with AT, inhibition stoichiometries of ~1−1.5 were observed for all FXa derivatives in the presence of pentasaccharide, suggesting that the reactivity of mutants with AT in the substrate pathway of the reaction has not been affected.

Amidolytic Activity. Kinetic parameters for the hydrolysis of the chromogenic substrates SpFXa and S2765 by the FXa derivatives are presented in Table 1. With the exception of the 220 loop mutants, all other mutants exhibited a wild type-like amidolytic activity, suggesting that the mutagenesis has most likely not adversely affected the catalytic pockets of FXa derivatives. In the case of the sodium loop mutants, however, both the K_m and k_{cat} of the S2765 hydrolysis were dramatically impaired (Table 1). Because of a better solubility of S2765, this chromogenic substrate was employed for the characterization of both 220−225Th and R221A/K222A/K224A mutants of FXa. Relative to wild-type FXa, the catalytic efficiencies of these mutants toward S2765 in TBS containing 0.1 M NaCl were impaired 1200- and 6000-fold, respectively. Increasing the concentration of Na^+ from 0.1 to 0.6 M markedly improved the amidolytic activity of these mutants (4−5-fold), suggesting that both mutants have also an impaired affinity for interaction with the metal ion. These results confirm the previous observations that the interaction of this loop with sodium plays a crucial role in the catalytic function of FXa (*31*, *32*).

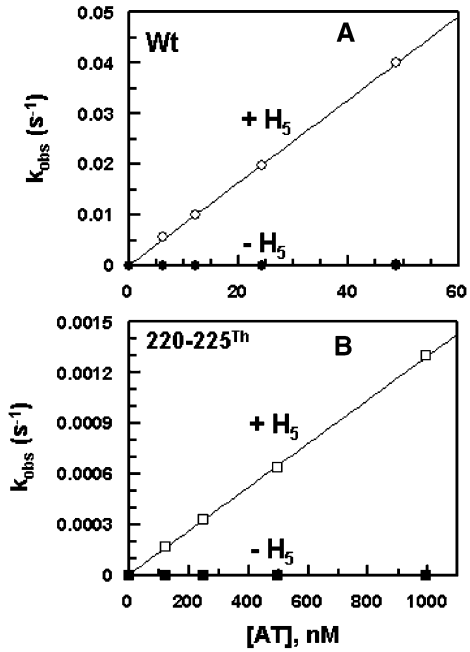

FIGURE 2: Dependence of the pseudo-first-order (k_{obs}) rate constants for the inhibition of wild type and the sodium loop mutant of FXa on AT concentrations in the absence and presence of pentasaccharide. (A) The k_{obs} values were determined from the time-dependent inhibition of wild-type FXa at different concentrations of the AT alone (●) or the AT−pentasaccharide complex (○) in TBS/Ca^{2+} at room temperature as described in Materials and Methods. (B) The same as panel A except that the k_{obs} values were determined for the sodium-binding 220−225Th mutant with AT alone (■) or the AT−pentasaccharide complex (□). Solid lines in both panels are best fits of kinetic data to the linear eq 1.

Inhibition by AT. The second-order rate constants (k_2) for both the noncatalyzed and pentasaccharide-catalyzed inhibition of FXa mutants by AT were determined from the slopes of linear plots of k_{obs} values as a function of the increasing concentrations of the serpin (Figure 2, shown for the wild type and 220−225Th mutant only) and presented in Table 2. AT inhibited wild-type FXa with k_2 values of 3.1×10^3 and 9.2×10^5 M^{-1} s^{-1} in the absence and presence of pentasaccharide, respectively. Consistent with the literature, these results suggested an ~300-fold rate accelerating effect for the cofactor in mediating FXa inhibition by AT (*9*). Similar to wild type, all three isosteric substitution mutants of the 39 loop exhibited similar reactivity with AT in both the absence and presence of the cofactor (Table 2). Thus, a similar 220−300-fold pentasaccharide-mediated conformational rate accelerating effect was observed with the AT inhibition of all three mutants of this loop. However, the E39A mutant reacted with AT with an ~2-fold impaired k_2,

Table 2: Inhibition of FXa Mutants by AT in the Absence and Presence of Pentasaccharide (H_5)[a]

	$-H_5 \times 10^3$ ($M^{-1}\,s^{-1}$)	$H_5 \times 10^5$ ($M^{-1}\,s^{-1}$)	H_5/$-H_5$ fold
WT FXa	3.1 ± 0.2	9.2 ± 0.4	297 ± 32
GD-FXa	2.6 ± 0.3	8.6 ± 0.5	331 ± 57
E36Q	2.7 ± 0.3	8.1 ± 0.6	300 ± 56
E37Q	2.1 ± 0.2	6.1 ± 0.8	290 ± 31
E39Q	2.5 ± 0.2	5.5 ± 0.3	220 ± 30
E39A	1.8 ± 0.2	4.2 ± 0.1	233 ± 31
Q61A	5.1 ± 0.1	10.4 ± 0.6	204 ± 16
K62E	4.0 ± 0.1	9.8 ± 0.3	245 ± 14
R63E	3.8 ± 0.1	8.6 ± 0.7	226 ± 24
R143A[b]	4.0 ± 0.1	5.7 ± 0.2	143 ± 9
K147A[b]	4.3 ± 0.1	9.6 ± 0.5	223 ± 17
R150A[b]	1.6 ± 0.1	0.88 ± 0.1	55 ± 10
R154A[b]	2.1 ± 0.1	4.8 ± 0.4	229 ± 30
$220-225^{Th}$	0.002 ± 0.0002	0.013 ± 0.001	650 ± 115
R221A/ K222A/ K224A	0.0007 ± 0.0001	0.0026 ± 0.0003	371 ± 96

[a] The second-order association rate constants for the AT inhibition of FXa derivatives in both the absence and presence of pentasaccharide (H_5) were determined by a discontinuous assay in TBS/Ca^{2+} at room temperature as described under Materials and Methods. All values are averages of at least three independent measurements ± SD. [b] The values are derived from ref *20*.

Table 3: Inhibition of FXa Mutants and Thrombin by AT K403T in the Absence and Presence of Pentasaccharide (H_5)[a]

	$-H_5 \times 10^2$ ($M^{-1}\,s^{-1}$)	$H_5 \times 10^5$ ($M^{-1}\,s^{-1}$)	H_5/$-H_5$ fold
WT FXa	4.1 ± 0.2	3.3 ± 0.1	805 ± 64
E36Q	3.5 ± 0.3	2.5 ± 0.1	714 ± 90
E37Q	3.8 ± 0.5	2.6 ± 0.1	684 ± 116
E39Q	5.3 ± 0.3	3.0 ± 0.2	566 ± 70
E39A	5.4 ± 0.6	3.3 ± 0.1	611 ± 86
thrombin	23.9 ± 1.1	0.18 ± 0.02	7.5 ± 1.2

[a] The second-order association rate constants for the AT inhibition of proteases in both the absence and presence of pentasaccharide (H_5) were determined by a discontinuous assay in TBS/Ca^{2+} at room temperature as described under Materials and Methods. All values are averages of at least three independent measurements ± SD.

suggesting that this residue may slightly contribute to the specificity of the AT reaction. However, the reactivity of the E39A mutant with AT was also impaired by the same extent in the presence of pentasaccharide; thus, a similar 233-fold rate enhancement for the cofactor-mediated AT inhibition of the mutant was also observed (Table 2). These results suggest that Glu^{39} is not specific for interaction with the heparin-activated AT, but it interacts with both the native and activated conformations of AT.

Recently, a molecular model of the activated AT−FXa Michaelis complex based on the structure of the heparin cofactor II−thrombin Michaelis complex was constructed, which predicts an interaction between the 39 loop of FXa with basic residues Lys^{403} and Arg^{406} on the activated AT (*23*). To test this model, the reactivity of wild type and 39 loop mutants of FXa with the K403T mutant of AT was studied in both the absence and presence of pentasaccharide. The results which are presented in Table 3 suggest that the reactivity of both wild type and the 39 loop mutants of FXa with the AT mutant is markedly impaired in the absence of the cofactor. Unlike an ~2-fold impairment in the reactivity of E39A with AT (Table 2), the reactivity of both wild type and FXa mutant with the AT mutant was comparable (Table 3). Similarly, in the presence of pentasaccharide, all FXa derivatives reacted with the AT mutant with similar k_2 values resulting in a similar improvement in the rate-accelerating effect of the cofactor for the mutant AT inhibition of wild type and all mutant proteases. Thus, the results presented in Table 3 suggest that the interaction of the 39 loop with Lys^{403}, if any, may be specific for the native, but not the activated serpin. It is worth noting that the underlying defect of the AT mutant with FXa derivatives may not be specific for a loss of interaction between 39 loop of FXa with Lys^{403} of the serpin, but rather due to a defect in the conformation of RCL in the mutant serpin. The observation that the reactivity of wild type, all four 39 loop mutants, and thrombin with the AT mutant was impaired, is consistent with this hypothesis (Table 3). This hypothesis is further supported by the observation that pentasaccharide, which has a minimal cofactor effect in the AT inhibition of thrombin, effectively accelerated the protease inhibition by the mutant serpin (Table 3). Previously, several natural variants of AT at the 402−407 region have been identified, which lead to AT deficiency (*33*). Mutations in this region of AT, which maps to the β-strand 1C and the polypeptide leading into s4B of the molecule, appear to relay structural changes to RCL and to the distal heparin binding site, so that the mutants have reduced heparin-binding and inhibitory activity (*33*). The observation that the K403A mutant also exhibited a reduced heparin affinity and inhibitory property is consistent with this hypothesis. The observation that pentasaccharide markedly enhanced the rate of thrombin inhibition by the mutant AT further confirms the hypothesis that the heparin-binding site of AT is allosterically linked to RCL and the strand 1 of β-sheet C of the serpin (*33*). Taken together, these mutagenesis data do not support a specific role for the 39 loop of FXa in interaction with the heparin-activated AT.

Role of 60 Loop in the FXa−AT Interaction. Loop 60 is known to make an important contribution to both the substrate and inhibitor specificity of thrombin (*34*, *35*). Unlike thrombin, however, this loop in FXa is significantly shorter, thus leaving the active site pocket open and readily accessible for target molecules (*36*). As shown in Table 2, the 60 loop mutants of FXa exhibited a slight improvement (less than 2-fold) with AT in the absence of the cofactor, possibly suggesting a repulsive interaction for this loop with the native serpin. However, the observation that pentasaccharide accelerated the rate of reaction greater than 200-fold with the AT inhibition of all three mutants suggests that the loop does not have a specific interactive site for the activated serpin and that the cofactor alleviation of a possible repulsive interaction between this loop with the activated serpin makes only a minor contribution to the acceleration of the reaction. Thus, our data do not support the results of a previous study proposing a major role for the specific interaction of Gln^{61} with the activated AT (*22*).

Role of the Na^+-Binding 220 Loop in FXa−AT Interaction. In contrast to 39 and 60 loop mutants, the reactivity of the sodium loop mutants of FXa with AT was impaired by 3−4 orders of magnitude (Table 2). On the basis of the X-ray crystal structure of FXa in complex with the recombinant tick anticoagulant peptide (*37*), a role for the positively charged residues of the sodium-binding loop with the activated conformation of AT has been postulated (*17*).

However, pentasaccharide accelerated the rate of inhibition of both FXa 220−225Th and FXa R221A/K222A/K224A mutants by AT, 650- and 371-fold, respectively (Figure 2 and Table 2), which suggests that the sodium-binding loop of FXa does not also make a specific interaction with the activated conformation of AT, although it plays a crucial role in interaction of FXa with AT in the native conformation. The observation that the amidolytic activities of the sodium loop mutants were also dramatically impaired suggests that the active-site pocket of the mutant proteases have been dramatically altered. This is consistent with previous reports that the conformation of the sodium loop is allosterically linked to the S1 and other sites in FXa and thus its mutagenesis adversely affects the structure and function of FXa (*32*, *38*). It should be noted that increasing the concentration of NaCl in TBS/Ca^{2+} to 0.5 M increased the reactivity of FXa mutants with AT ~2-fold. Under these conditions, the reactivity of the mutants with AT could not be accurately determined possibly due to the electrostatic nature of the AT−pentasaccharide interaction. However, on the basis of our previous results, we believe that sodium would also influence the reactivity of FXa with AT at a similar extent in both the native and activated conformations of the serpin (*32*).

AT inhibits FXa and other target serine proteases by a two-step reaction mechanism in which an enzyme−serpin encounter complex, formed in the initial reaction step, is converted to a stable, covalent complex in the second step of the reaction (*39*, *40*). To evaluate the kinetic step that is dramatically affected by the mutagenesis of the sodium loop, the pseudo-first-order rate constant (k_{obs}) for the AT inhibition of the R221A/K222A/K224A mutant was determined in the presence of increasing concentrations of the full-length high affinity heparin. Full-length heparins are known to lower the dissociation constant (K_D) for the formation of the initial enzyme−inhibitor encounter complex with a minimum effect on the rate constant (k) for formation of the stable, covalent complex (*39*). Generally, rapid kinetic methods are required to resolve the two-step reaction of AT with FXa and other coagulation proteases (*39*, *40*). In the case of the heparin-catalyzed reaction of AT with R221A/K222A/K224A, however, because the k value was dramatically impaired, high concentrations of the mutant serpin−heparin complexes could be employed in the reaction to measure kinetic values for both steps in a discontinuous assay method. As shown in Figure 3, in the presence of the full-length heparin, the k_{obs} values for reaction with the FXa mutant showed a saturable dependence on the concentration of the AT−heparin complex, indicating the saturation of an intermediate heparin−AT−protease encounter complex prior to formation of a stable, covalent complex (*39*). Nonlinear regression analysis of data by the hyperbolic eq 2 yielded K_D of 769 ± 160 nM for the ternary complex dissociation constants, and a k value of 0.014 ± 0.001 s^{-1} for the rate constant of the stable complex formation. Comparisons of these values with the corresponding values for the ternary wild-type FXa−AT−heparin protease complex, $K_D = 90$ nM and $k = 18$ s^{-1}, as determined previously by rapid kinetic methods (*41*), suggest that the defect of mutation is primarily due to greater than 3 orders of magnitude impairment in the rate constant of the second reaction step and less than an order of magnitude impairment in the K_D of the initial interaction.

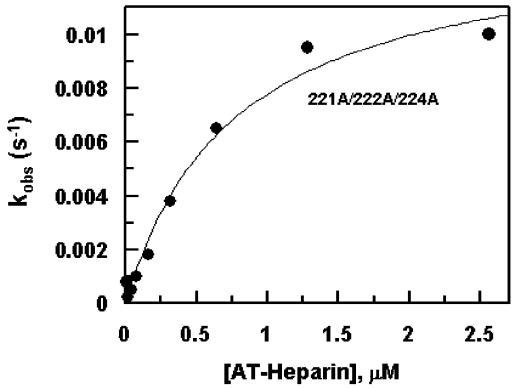

FIGURE 3: Dependence of the pseudo-first-order (k_{obs}) rate constants for the inhibition of the sodium-binding loop mutant of FXa on the AT−heparin complex concentrations. The k_{obs} values were determined from the time-dependent inhibition of the FXa mutant at different concentrations of the AT−heparin complex (x-axis) in TBS/Ca^{2+} at room temperature as described in Materials and Methods. Solid lines are best fits of data to the nonlinear eq 2.

Finally, unlike the three surface loops discussed above, in a previous mutagenesis study, we demonstrated that the basic residues of the autolysis loop are critical for the protease interaction with both the native and activated conformations of AT (*20*). Specifically, the substitution of Lys^{143} and Lys^{147} with Ala improved the reactivity of mutants with the native conformation of AT ~2-fold; however, the Ala substitution mutant of Arg^{150} exhibited an order of magnitude impairment with the serpin specifically in the activated conformation (*20*). Interestingly, the same result was also obtained with an $Arg^{150} \rightarrow$ Ala substitution mutant of FIXa, which similar to FXa, reacts differentially with the native and heparin-activated AT (*21*). The recent molecular model of the activated AT−FXa complex supported our mutagenesis data and further predicted that a salt bridge between Arg^{150} and Glu^{237} of AT can stabilize the serpin−protease complex (*23*). However, Glu^{237} is located on the strand 4 of β-sheet C, a site distinct from the strand 3 of β-sheet C, which has been recently identified as the target exosite on AT, made accessible for the protease interaction by pentasaccharide (*18*). The strand 3 of β-sheet C contains an acidic residue (Glu^{255}), which can also interact with Arg^{150} in the activated conformation of the serpin. Both structural and mutagenesis data have indicated that Glu^{255} is involved in a weak electrostatic interaction with the P1 Arg^{393} of AT in the native, but not in the activated conformation of the serpin (*8*, *42*). The disruption of this ionic interaction by the conformational activation of AT by heparin leads to an ~5-fold acceleration of the protease inhibition by the activated serpin (*42*). Thus, it is possible that the conformational activation of the serpin by heparin switches the intramolecular interaction between Glu^{255} and Arg^{393} to an intermolecular interaction between Glu^{255} (or Glu^{237}) of AT and Arg^{150} of FXa. Thus, such pentasaccharide-mediated interactions, together with a minor effect arising from the cofactor alleviating the repulsive interaction of the basic loop 60 of FXa with a basic site of the serpin (*23*), may primarily be responsible for the differential reactivity of FXa with the native and activated conformations of AT.

ACKNOWLEDGMENT

We would like to thank Audrey Rezaie for proofreading of the manuscript.

REFERENCES

1. Schechter, I., and Berger, A. (1967) On the size of the active site in proteases. I. Papain. *Biochem. Biophys. Res. Commun. 27*, 157−162.
2. Mann, K. G., Jenny, R. J., and Krishnaswamy, S. (1988) Cofactor proteins in the assembly and expression of blood clotting enzyme complexes. *Annu. Rev. Biochem. 57*, 915−956.
3. Rosing, J., Tans, G., Govers-Riemslag, J. W. P., Zwaal, R. F. A. Z., and Hemker, H. C. (1980) The role of phospholipids and factor Va in the prothrombinase complex. *J. Biol. Chem. 255*, 274−283.
4. Damus, P. S., Hicks, M., and Rosenberg, R. D. (1973) Anticoagulant action of heparin. *Nature 246*, 355−357.
5. Carrell, R. W., Evans, D. L., and Stein, P. E. (1991) Mobile reactive centre of serpins and the control of thrombosis. *Nature 353*, 576−578.
6. Olson, S. T., and Björk, I. (1992) Regulation of thrombin by antithrombin and heparin cofactor II in *Thrombin: Structure and Function* (Berliner, L. J., Ed) pp 159−217, Plenum Press, New York.
7. Rosenberg, R. D., and de Agostini, A. I. (1991) New approaches for defining sequence specific synthesis of heparin sulfate chains. *Adv. Exp. Med. Biol. 313*, 307−316.
8. Jin, L., Abrahams, J., Skinner, R., Petitou, M., Pike, R. N., and Carrell, R. W. (1997) The anticoagulant activation of antithrombin by heparin. *Proc. Natl. Acad. Sci., U.S.A. 94*, 14683−14688.
9. Olson, S. T., Björk, I., Sheffer, R., Craig, P. A., Shore, J. D., and Choay, J. (1992) Role of the antithrombin-binding pentasaccharide in heparin acceleration of antithrombin-proteinase reactions. Resolution of the antithrombin conformational change contribution to heparin rate enhancement. *J. Biol. Chem. 267*, 12528−12538.
10. Yang, L., Manithody, C., and Rezaie, A. R. (2002) Localization of the heparin binding exosite of factor IXa. *J. Biol. Chem. 277*, 50756−50760.
11. Bedsted, T., Swanson, R., Chuang, Y.-J., Bock, P. E., Björk, I., and Olson, S. T. (2003) Heparin and calcium ions dramatically enhance antithrombin reactivity with factor IXa by generating new interaction exosites. *Biochemistry 42*, 8143−8152.
12. Skinner, R., Abrahams, J., Whisstock, J. C., Lesk, A. M., Carrell, R. W., and Wardell, M. R. (1997) The 2.6 Å structure of antithrombin indicates a conformational change at the heparin binding site. *J. Mol. Biol. 266*, 601−609.
13. Huntington, J. A., Olson, S. T., Fan, B., and Gettins, P. G. W. (1996) Mechanism of heparin activation of antithrombin. Evidence for reactive center loop preinsertion with expulsion upon heparin binding. *Biochemistry 35*, 8495−8503.
14. Huntington, J. A., and Gettins, P. G. W. (1998) Conformational conversion of antithrombin to a fully activated substrate of factor Xa without need for heparin. *Biochemistry 37*, 3272−3277.
15. Pike, R. N., Potempa, J., Skinner, R., Fitton, H. L., McGraw, W. T., Travis, J., Owen, M., Jin, L., and Carrell, R. W. (1997) Heparin-dependent modification of the reactive center arginine of antithrombin and consequent increase in heparin binding affinity. *J. Biol. Chem. 272*, 19652−19655.
16. Huntington, J. A., McCoy, A., Belzar, K. J., Pei, X. Y., Gettins, P. G. W., and Carrell, R. W. (2000) The conformational activation of antithrombin. *J. Biol. Chem. 275*, 15377−15383.
17. Chuang, Y.-J., Swanson, R., Raja, S. M., and Olson, S. T. (2001) Heparin enhances the specificity of antithrombin for thrombin and factor Xa independent of the reactive center loop sequence. *J. Biol. Chem. 276*, 14961−14971.
18. Izaguirre, G., Zhang, W., Swanson, R., Bedsted, T., and Olson, S. T. (2003) Localization of an antithrombin exosite which promotes rapid inhibition of factors Xa and IXa dependent on heparin activation of the serpin. *J. Biol. Chem. 278*, 51433−51440.
19. Bode, W., Mayr, I., Baumann, U., Huber, R., Stone, S. R., and Hofsteenge, J. (1989) The refined 1.9 Å crystal structure of human α-thrombin: interaction with D-Phe-Pro-Arg chloromethyl ketone and significance of the Tyr-Pro-Pro-Trp insertion segment. *EMBO J. 8*, 3467−3475.
20. Manithody, C., Yang, L., and Rezaie, A. R. (2002) Role of basic residues of the autolysis loop in the catalytic function of factor Xa. *Biochemistry 41*, 6780−6788.
21. Yang, L., Manithody, C., Olson, S. T., and Rezaie, A. R. (2003) Contribution of basic residues of the autolysis loop to the substrate and inhibitor specificity of factor IXa. *J. Biol. Chem. 278*, 25032−25038.
22. Quinsey, N. S., Whisstock, J. C., Le Bonniec, B., Louvain, V., Bottomley, S. P., and Pike, R. N. (2002) Molecular determinants of mechanism underlying acceleration of the interaction between antithrombin and factor Xa by heparin pentasaccharide. *J. Biol. Chem. 277*, 15971−15978.
23. Huntington, J. A. (2003) Mechanisms of glycosaminoglycan activation of the serpins in hemostasis. *Thromb. Haemostasis 1*, 1535−1549.
24. Rezaie, A. R., Neuenschwander, P. F., Morrissey, J. H., and Esmon, C. T. (1993) Analysis of the functions of the first epidermal growth factor-like domain of factor X. *J. Biol. Chem. 268*, 8176−8180.
25. Rezaie, A. R., and Yang, L. (2001) Probing the molecular basis of factor Xa specificity by mutagenesis of the serpin, antithrombin. *Biochim. Biophys. Acta 1528*, 167−176.
26. Rezaie, A. R. (1996) Role of residue 99 at the S2 subsite of factor Xa and activated protein C in enzyme specificity. *J. Biol. Chem. 271*, 23807−23814.
27. Olson, S. T., Björk, I., and Shore, J. D. (1993) Kinetic characterization of heparin-catalyzed and uncatalyzed inhibition of blood coagulation proteinases by antithrombin. *Methods Enzymol. 222*, 525−560.
28. Rezaie, A. R. (2002) Insight into the molecular basis of coagulation proteinase specificity by the mutagenesis of the serpin antithrombin. *Biochemistry 41*, 12179−12185.
29. Rezaie, A. R. (2000) Heparin binding exosite of factor Xa. *Trends Cardiovasc. Med. 10*, 333−338.
30. Rezaie, A. R. (1998) Calcium enhances heparin catalysis of the antithrombin-factor Xa reaction by a template mechanism. Evidence that calcium alleviates Gla-domain antagonism of heparin binding to factor Xa. *J. Biol. Chem. 273*, 16824−16827.
31. Dang, Q. D., and Di Cera, E. (1996) Residue 225 determines the Na^+-induced allosteric regulation of catalytic activity in serine proteases. *Proc. Natl. Acad. Sci., U.S.A. 93*, 10653−10656.
32. Rezaie, A. R., and He, X. (2000) Sodium binding site of factor Xa: Role of sodium in the prothrombinase complex. *Biochemistry 39*, 1817−1825.
33. Lane, D. A., Olds, R. R., and Thein, S.-L. (1992) Antithrombin and its deficiency states. *Blood Coagulation Fibrinolysis 3*, 315−341.
34. Le Bonniec, B. F., Guinto, E. R., MacGillivray, R. T. A., Stone, S. R., and Esmon, C. T. (1993) The role of thrombin's Tyr-Pro-Pro-Trp motif in the interaction with fibrinogen, thrombomodulin, protein C, antithrombin III and the Kunitz inhibitors. *J. Biol. Chem. 268*, 19055−19061.
35. Rezaie, A. R. (1996) Tryptophan60-D in the B-insertion loop of thrombin modulates the thrombin-antithrombin reaction. *Biochemistry 35*, 1918−1924.
36. Padmanabhan, K., Padmanabhan, K. P., Tulinsky, A., Park, C. H., Bode, W., Huber, R., Blankenship, D. T., Cardin, A. D., and Kisiel, W. (1993) Structure of human des (1−45) factor Xa at 2•2 Å resolution. *J. Mol. Biol. 232*, 947−966.
37. Wei, A., Alexander, R. S., Duke, J., Ross, H., Rosenfeld, S. A., and Chang, C.-H. (1998) Unexpected binding mode of tick anticoagulant peptide complexed to bovine factor Xa. *J. Mol. Biol. 283*, 147−154.
38. Camire, R. M. (2002) Prothrombinase assembly and S1 site occupancy restore the catalytic activity of FXa impaired by mutation at the sodium-binding site. *J. Biol. Chem. 277*, 37863−37870.
39. Olson, S. T., and Shore, J. D. (1982) Demonstration of a two-step reaction mechanism for inhibition of α-thrombin by antithrombin III and identification of the step affected by heparin. *J. Biol. Chem. 257*, 14891−14895.
40. Craig, P. A., Olson, S. T., and Shore, J. D. (1989) Transient kinetics of heparin-catalyzed protease inactivation by antithrombin III: characterization of assembly, product formation and heparin

dissociation in the factor Xa reaction. *J. Biol. Chem. 264*, 5452−5461.
41. Rezaie, A. R., and Olson, S. T. (2000) Calcium enhances heparin catalysis of the antithrombin-factor Xa reaction by promoting the assembly of an intermediate heparin-antithrombin-factor Xa binding complex. Demonstration by rapid kinetics studies. *Biochemistry 39*, 12083−12090.
42. Jairajpuri, M. A., Lu, A., and Bock, S. C. (2002) Elimination of P1 arginine 393 interaction with underlying glutamic acid 255 partially activates antithrombin III for thrombin inhibition but not factor Xa inhibition. *J. Biol. Chem. 277*, 24460−24465.

BI036145A